MOLECULAR ECOLOGY

Molecular Ecology (2010) **19**, 1994–2010 doi: 10.1111/j.1365-294X.2010.04626.x

World phylogeography and male-mediated gene flow in the sandbar shark, *Carcharhinus plumbeus*

DAVID S. PORTNOY,* JAN R. MCDOWELL,† EDWARD J. HEIST,‡ JOHN A. MUSICK† and JOHN E. GRAVES†

**Department of Wildlife and Fisheries, Texas A&M University, TAMU 2258, College Station, TX 77843-2258, USA, †Virginia Institute of Marine Science, College of William and Mary, PO Box 1346, Gloucester Point, VA 23062-1346, USA, ‡Southern Illinois University, 1125 Lincoln Drive, Carbondale, IL 62901-6511, USA*

Abstract

The sandbar shark, *Carcharhinus plumbeus*, is a large, cosmopolitan, coastal species. Females are thought to show philopatry to nursery grounds while males potentially migrate long distances, creating an opportunity for male-mediated gene flow that may lead to discordance in patterns revealed by mitochondrial DNA (mtDNA) and nuclear markers. While this dynamic has been investigated in elasmobranchs over small spatial scales, it has not been examined at a global level. We examined patterns of historical phylogeography and contemporary gene flow by genotyping 329 individuals from nine locations throughout the species' range at eight nuclear microsatellite markers and sequencing the complete mtDNA control region. Pairwise comparisons often resulted in fixation indices and divergence estimates of greater magnitude using mtDNA sequence data than microsatellite data. In addition, multiple methods of estimation suggested fewer populations based on microsatellite loci than on mtDNA sequence data. Coalescent analyses suggest divergence and restricted migration among Hawaii, Taiwan, eastern and western Australia using mtDNA sequence data and no divergence and high migration rates, between Taiwan and both Australian sites using microsatellite data. Evidence of secondary contact was detected between several localities and appears to be discreet in time rather than continuous. Collectively, these data suggest complex spatial/temporal relationships between shark populations that may feature pulses of female dispersal and more continuous male-mediated gene flow.

Keywords: contemporary gene flow, dispersal potential, elasmobranch, historical biogeography, philopatry

Received 24 March 2009; revision received 9 February 2010; accepted 21 February 2010

Introduction

Molecular phylogeographic studies aim to shed light on the historical mechanisms and processes that have led to the current distribution of genetic variation within species (Avise 2000). At the same time, these studies provide information about current population structure and gene flow, which is important for management and conservation (Graves 1998). The marine environment is a challenging arena for such study, as the obvious vicariant boundaries found in terrestrial environments are often lacking. This poses problems both in terms of sample design and the analysis and interpretation of results (Waples 1998). In addition, many marine organisms have life histories that allow for long distance dispersal during one or more life stages (Palumbi *et al.* 1997). Despite this potential for gene flow, the use of high-resolution molecular markers, like mitochondrial DNA (mtDNA) sequence data and nuclear microsatellite loci, has demonstrated that there may be cryptic boundaries and fine scale population structure in the marine environment (Avise 1998; Graves 1998). In species where different male and female reproductive strategies have led to differences in dispersal potential, the situation may be more complex. To resolve historical

Correspondence: David S. Portnoy, Fax: +1 804 684 7157; E-mail: dsport@tamu.edu

and contemporary patterns of biogeography in these species, multiple markers with different modes of inheritance need to be examined (Karl *et al.* 1992; Palumbi & Baker 1994).

In sharks, male and female dispersal potentials often differ. Many species use nursery areas to increases the survival of their progeny, presumably by providing young sharks with an array of prey species and more importantly, reduced densities of elasmobranch predators (Springer 1967; Branstetter 1990). This increased juvenile survival has likely led to selection for female philopatry, which has been documented for several species (Pratt & Carrier 2001; Feldheim *et al.* 2002; Chapman *et al.* 2009). This selection pressure may be particularly high in live-bearing sharks, as females balance the increased costs of parental investment with the benefit of increased lifetime reproductive success. Males have very little parental investment and therefore may be less likely to show philopatry to breeding and nursery areas.

The sandbar shark, *Carcharhinus plumbeus*, is a large, cosmopolitan, discontinuously distributed, coastal species found in warm temperate and sub-tropical waters and is exploited throughout most of its range. It is distributed throughout the Atlantic, Pacific and Indian oceans, though it is believed to be absent from the expanse of Oceania between New Caledonia and the Hawaiian archipelago (Compagno *et al.* 2005). The species has also been reported in the eastern Pacific near the Revillagigedo and Galapagos Islands, but these reports are likely cases of mistaken identity (J. Musick, personal observation).

Springer (1960) suggested that the sandbar shark may be capable of transoceanic migrations and several lines of evidence support this view. First, previous studies have suggested that sandbar sharks found in the western North Atlantic and Gulf of Mexico form one panmictic population with mating grounds off the coast of southern Florida (Springer 1960; Heist *et al.* 1995). Since nursery grounds are found as far north as Cape Cod, Massachusetts (Castro 1993), some females migrate distances of up to 1600 km to give birth. Second, individually tagged sandbar sharks have been recaptured at distances of over 3000 km from the original site of capture (Kohler & Turner 2001).

There are also reasons to expect that transoceanic migrants are more likely to be male than female in sandbar sharks. The use of nursery areas by females suggests that this species, like other elasmobranchs, may show female philopatry. For shark species in which mating occurs on or near nursery grounds, males may remain in the vicinity to ensure opportunities for copulation (Pratt & Carrier 2001). In sandbar sharks, however, mating occurs at locations remote from nursery grounds. At all other times the sexes are segregated and males tend to be found further offshore (Springer 1960).

In this study we characterize microsatellite and mtDNA control region variation within and between putative populations of sandbar sharks worldwide. Discordance in observed patterns of variation across samples based on different classes of molecular markers are used to look for evidence of sex biased dispersal and coalescent based approaches are used to elucidate the role that sex biased dispersal may have in shaping the global distribution of marine species. The questions posed are crucial for conservation and management of the species, as the sandbar shark is a principal target of commercial shark fisheries throughout most of its range (McAuley *et al.* 2007). In the western North Atlantic overexploitation has lead to a closure of the fishery (NOAA 2008).

Materials and methods

Sample collection, extraction, genotyping and sequencing

Muscle tissue or fin clips were collected from sharks in the Pacific Ocean; Hawaii (HI), Taiwan (TW) and Eastern Australia (EAUS), the Indian Ocean; South Africa (SAFR) and Western Australia (WAUS) and the Atlantic Ocean; Delaware Bay (DEL), Chesapeake Bay (CB), Eastern Shore lagoons of Virginia (ES) and the Gulf of Mexico (GOM) (Fig. 1). All samples were collected between 2002–2006 except for historical samples from GOM, which were collected in 1991 and 1993 and samples from WAUS, which were collected in 1999. Tissue was stored either in 95% ethanol or 10% DMSO buffer (Seutin *et al.* 1991) at 4 °C until extraction. DNA was isolated using a Chelex extraction protocol (Estoup *et al.* 1996). After a 2 min centrifugation at 16 000 *g*, 0.3 μL of the supernatant was used as a template for PCR reactions.

Eight microsatellite markers were amplified for each individual using IRD-700 and IRD-800 (LiCor, Lincoln NE) labelled forward primers. Descriptions of primers and PCR conditions for the six species-specific markers, Cpl-53, *Cpl*-90, *Cpl*-128, *Cpl*-132, *Cpl*-166, and *Cpl*-169 are reported elsewhere (Portnoy *et al.* 2006, 2007). Two additional markers, *Cli*-12 and *Cli*-103, isolated from the congeneric blacktip shark, *Carcharhinus limbatus*, were amplified following protocols outlined in Keeney & Heist (2003). All amplicons were electrophoresed through 25 cm 6.5% polyacrylamide gels using a LiCor 4200 Global IR^2 system. A 50–350 bp size standard was run in the first, middle and last lanes of each gel and locus-specific standards were run in every fourth lane.

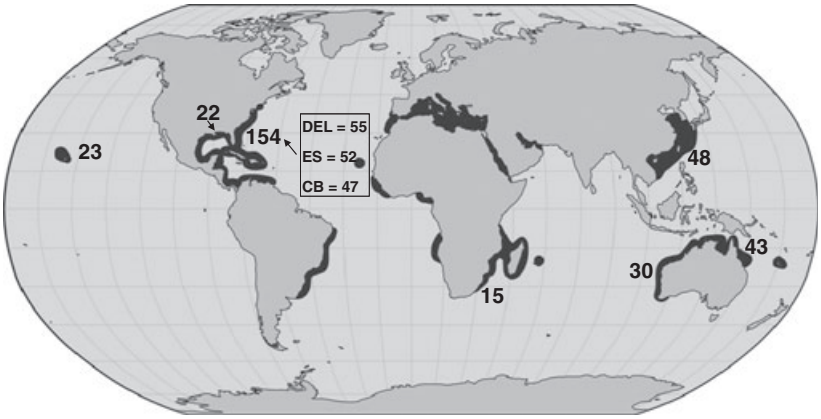

Fig. 1 Map of worldwide sampling locations of sandbar sharks. The sampling effort is printed in bolded numbers, the distribution of species is in shadow. The map was adapted from Compagno *et al.* (2005). DEL: Delaware Bay; CB: Chespeake Bay; ES: Eastern Shore lagoons of Virginia.

Alleles were scored manually with the aid of Gene ImagIR 4.05 (Scanalytics, Rockville, MD, USA). Twenty-five percent of samples were haphazardly selected, re-amplified and rescored to ensure consistent scoring. Individuals for which more than two loci could not be reproducibly scored were discarded.

The entire mitochondrial control region (1665–1668 bp) was amplified using the primer Pro-L (5′-AGGGRAAGGAGGGTCAAACT-3′), which is complementary to a portion of the proline tRNA located on the light strand and the primer 282H (5′-AAFGCTAFFACCAAACCT-3′), a portion of the 12S rRNA on the heavy strand (Keeney *et al.* 2003). Twenty-five microlitres of PCR reactions contained 20 mM Tris–HCl (pH 8.4), 1.5 mM $MgCl_2$, 1 μg/μL BSA, 0.2 mM dNTP mix, 25 pmol of each primer, 2 μL of template and 0.025 U/μL *Taq* polymerase. Reaction conditions consisted of an initial denaturation at 95 °C for 4 min followed by 35 cycles at 95 °C for 1 min, 61 °C for 0.5 min and 72 °C for 1 min, followed by a final extension of 72 °C for 10 min. PCR products were purified using Qiagen Qiaquick PCR purification kits (Qiagen, Valencia CA, USA). To ensure accurate sequencing of rare haplotypes, internal primers, which when paired with the original primers amplified overlapping fragments, were also developed, CP5′R : (5′-ACCTTAATGAACCAGATGAGCC-3′) and CP3′F: (5′-CCTTTAATGGCATATTTATCC-3′). PCR conditions were as described above except that that Pro-L 5′ and CP5′R annealing was at 64.5 °C for 0.75 min and for CP3′F and 282H annealing was at 61.5 °C for 0.5 min.

Purified products were sequenced in the forward and reverse direction using BigDye Terminator v.3.1 Cycle Sequencing Kit (Applied Biosystems Inc., Warrington, UK). Five microlitres of sequencing reactions consisted of 10–40 ng of template, 0.5 μL of BigDye master mix, 1 μL of BigDye 5 × Reaction Buffer and 32 pmol of F or R primer. Sequencing conditions consisted of a denaturation at 96 °C for 1 min followed by 25 cycles at 96 °C for 10 s, 50 °C for 5 s and 60 °C for 4 min. Amplifications were electrophoresed on an ABI 3130xl (Applied Biosystems Inc., Warrington, UK) sequencer through 70 cm capillaries. Results were scored using SEQUENCING ANALYSIS v.5.2 software (Applied Biosystems Inc., Warrington, UK). The resultant SCF curves were imported into SEQUENCHER v.3.0 (Gene Codes Corp., Ann Arbor, MI, USA) where consensus sequences of the entire control region were formed by combining reverse and forward sequences. All consensus sequences were aligned in MACVECTOR v.8.1.1 (Accelrys Inc. San Diego, CA, USA) using the ClustalW algorithm (Thompson *et al.* 1994).

Summary statistics

Conformance to the expectations of Hardy–Weinberg equilibrium was calculated for each microsatellite locus and population in GENEPOP v.4.0 (Raymond & Rousset 1995; Rousset 2008) using exact tests with 10 000 iterations. Expected and observed numbers of heterozygotes were also calculated in GENEPOP. Number of alleles, allele frequencies and allelic richness were calculated for each locus and putative population with FSTAT v.2.9.3.2 (Goudet 2001). MICRO-CHECKER v.2.2.3 (Van Oosterhout *et al.* 2004) was used to screen for null alleles and genotyping error.

For control region sequences, nucleon diversity (h), nucleotide diversity (π), number of polymorphic sites (s), base composition and the number of transitions, transversions and indels were calculated for each population in ARLEQUIN v.3.11 (Excoffier *et al.* 2005).

Population structure

For both microsatellites and control region sequence data, genetic diversity within and among populations and ocean basins (defined as the Atlantic and Indian/-Pacific) was estimated using an analysis of molecular variance (AMOVA; Excoffier *et al.* 1992) implemented in

ARLEQUIN with 10 000 permutations (Excoffier *et al.* 2005). Pairwise F_{ST} values were calculated from microsatellite data and pairwise Φ_{ST} values were calculated from mtDNA sequence data in ARLEQUIN with 10 000 permutations. Significance was assessed at the 0.05 and 0.01 level after correction for multiple testing using a sequential Bonferroni adjustment (Rice 1989).

Since nuclear and mtDNA loci have different modes of inheritance and mtDNA is haploid, one would expect discordant pairwise F_{ST} (Φ_{ST}) values (Buonaccorsi *et al.* 2001). In addition, F_{ST} values from very polymorphic microsatellite loci are expected to be small, as F_{ST} values cannot exceed the homozygosity of the markers used (Hedrick 1999). To address this issue Jost's *D*, an unbiased estimator of divergence (Jost 2008), was calculated for mtDNA data using SPADE (available at http://chao.stat.nthu.edu.tw/softwareCE.html) and for nuclear data using SMOGD (Crawford 2009), allowing for direct comparison. A Mantel test (Smouse *et al.* 1986), implemented in Arlequin with 10 000 permutations, was then used to evaluate whether divergence estimates between marker types were correlated, indicating that observed differences were due to characteristics of the markers or truly incongruent, indicating sex biased dispersal. For the Mantel test only one Atlantic sample was included as pairwise F_{ST} and Φ_{ST} values between all Atlantic samples indicated that these samples represent a single population.

Bayesian multi-locus clustering was implemented in Structure v.2.2 (Falush *et al.* 2007, http://pritch.bsd.uchicago.edu/structure.html). This software uses multilocus genotype data to detect distinct populations and assign individuals to these populations. The method is flexible, allowing for identification of the number of populations within the data irrespective of geographic origin of samples. Simulations were run with a burn-in period of 100 000 steps followed by an additional 100 000 steps. The number of populations was set to two, three, four, five, six and seven with five replicates for each. The probability of k populations was then calculated from the average of five replicates.

SAMOVA (v. 1.0, http://cmpg.unibe.ch/software/samova/) is an approach developed by Dupanloup *et al.* (2002) that detects genetic barriers in a sampling region and defines a partition (or partitions) of the set of populations sampled within groups of populations that are maximally differentiated from each other. The approach used by SAMOVA differs from the Bayesian clustering implemented in Structure in that assignment of individuals to populations or groups of populations is based on genetic distance between/among groups and does not assume either Hardy-Weinberg equilibrium or genotypic equilibrium between loci within populations. It also allows for the analysis of both microsatellite and mtDNA sequence data. Sampling locations were analysed as groups of two, three, four, five, six and seven using 100 simulated annealing processes.

To visualize the relationship between populations using microsatellite data, correspondence analysis (Guinand 1996) was implemented in GENETIX v.4.05.2 (Belkhir *et al.* 2004). In addition, Network v.4.510 (Fluxus-engineering.com) was used to create minimum spanning networks from mtDNA sequence data using the full median joining algorithm (Bandelt *et al.* 1999). Maximum parsimony (MP) analysis was used to remove unnecessary alternate connections (Polzin & Daneshmand 2003). Support for the most common connections found across Steiner trees was calculated by evaluating the percentage of Steiner trees in which they appeared.

Gene flow

To investigate patterns of gene flow, relative rates of long term migration between the 6 populations defined by mtDNA analysis were evaluated via the maximum-likelihood coalescent approach implemented in Migrate V.2.4.2 (Beerli & Felsenstein 2001; http://popgen.dcd.fsu.edu/Migrate-n.html) using microsatellite data. Preliminary analyses were used to estimate priors for M and θ for use in a series of final runs. Three final simulations with different starting points were run with 10 short chains (500 trees sampled) and three long chains (10 000 trees sampled). For each chain the first 10 000 steps were used as a burn-in and adaptive heating was used to ensure an independent, comprehensive search of parameter space.

To further examine relationships between populations showing discordant results between marker types, IMA (Hey & Nielsen 2007), which uses a Bayesian MCMC method, was used to estimate *t* (mutation scaled time since divergence) and *m* (mutation scaled migration rate) for five pairs of populations (TW_WAUS, TW_EAUS, EAUS_WAUS, HI_TW and HI_EAUS). SAFR was excluded from these analyses because of small sample size. HI was included because it showed clear divergence from the other three populations with both marker types. A comparison between WAUS and HI was excluded because there is no direct route for migration between the localities. Analyses were run using both mtDNA and microsatellite data for all pairs of populations. In addition, mtDNA data for Atlantic samples were pooled and analysed with pooled Pacific samples to provide a relative measure of mtDNA divergence time that could be compared with the other runs. A series of preliminary runs was used to determine priors for subsequent runs. Final runs incorporating these priors were duplicated with different starting points to ensure that independent runs converged. Final

runs consisted of a burn-in period of at least 500 000 generations and a post-burn-in of at least 10 000 000 generations. Each run included 10 chains with geometric heating.

The model behind IMa assumes that each population is panmictic and that the genealogical relationship between each pair of populations is unaffected by input from other populations. While neither assumption is likely correct, the model is still able to distinguish between complete isolation and divergence with gene flow (Machado *et al.* 2002; Won & Hey 2005; Niemiller *et al.* 2008). For each pairwise comparison, three possibilities were considered; high gene flow in the present or near present, gene flow after divergence in the past and divergence and isolation. First, posterior probability distributions of t were examined to evaluate the probability of zero time since divergence, indicating a lack of divergence (J. Hey, personal communication), which may be caused by high gene flow in the recent past or present. For comparisons with non-zero divergence, posterior probability distributions of m were examined to evaluate the probability of zero gene flow, indicating isolation (Won & Hey 2005; Niemiller *et al.* 2008). For distributions of m where the probability of zero was similar to the peak probability or the location of the distributions peak was close to zero, log likelihood ratio tests were used to examine whether a null model with zero gene flow fit the data (Hey & Nielsen 2007). When analysis indicated gene flow, the distribution of migration events over time was also evaluated to determine whether gene flow was likely contemporary or in the past and whether it was continuous or discrete (Won & Hey 2005; Niemiller *et al.* 2008). Distributions of all parameter estimates were left in a mutation scaled format due to uncertainty caused by violations of the assumptions of the model (Wakeley 2000; Strasburg & Rieseberg 2009) and the lack of reliable estimates of mutation rates for microsatellites in sharks.

Results

Summary statistics

A total of 329 individuals from nine localities was genotyped at eight microsatellite loci. After correction for multiple tests, the genotypes at one locus in one location (*Cpl*-53, WAUS) deviated significantly from the expectations of Hardy–Weinberg equilibrium ($P = 0.002$; Table 1). This was due to an excess of homozygotes; the Micro-Checker software confirmed that this locus showed signs of null alleles. Pairwise comparisons between WAUS and other regions were therefore run with and without *Cpl*-53. The least polymorphic locus was *Cpl*-53, which had 10 alleles and the most polymorphic locus was *Cpl*-166, which had 64 alleles. Allelic richness averaged across loci was greatest in the SAFR and TW collections, 13.28 and 13.11 respectively. Individual Atlantic collections had lower average allelic richness values than Pacific collections, except for HI, which had the smallest average allelic richness value of any sample (8.45; Table 2).

A total of 67 mtDNA haplotypes (Genbank accession GU724517–GU724583) was found across all samples. The control region varied in size from 1065 bp in some Pacific samples to 1068 bp in some Atlantic samples. This size heterogeneity was due largely to indels in long strings of adenine found at the 3′ end of the sequence. The control region was composed of 13.7% guanine, 35.4% thymine, 31.0% adenine and 19.8% cytosine. There were 39 variable sites, eight transversions, 26 transitions and five indels (Electronic Appendix A). Of the 67 haplotypes, 32 were in the Indo-Pacific region, eight were in the western Indian Ocean and 29 were in the Atlantic Ocean. Of these, two haplotypes were shared between the Indian and the Atlantic Oceans. Total nucleon (haplotype) diversity (h) was 0.959 and nucleotide diversity (π) was 0.00475. Haplotype diversity was highest in Atlantic samples and smallest in HI and EAUS. Summary statistics for each population and across all populations are presented in Table 2.

Population structure

The AMOVA analysis of the mtDNA sequence data detected significant population structure with significant components of variance within and between ocean basins ($\Phi_{SC} = 0.2066$, $\%V = 8.98$, $P < 0.0001$ and $\Phi_{CT} = 0.5654$, $\%V = 56.54$, $P = 0.0075$, Table 3). Pairwise comparisons using mtDNA sequences showed no significant differentiation between collection sites in the Atlantic Ocean after correction for multiple tests. However, Atlantic Ocean sites were significantly differentiated from all Pacific and Indian Ocean sites after correction for multiple tests ($P \leq 0.01$). All Pacific and Indian Ocean sites were also significantly differentiated from each other after correction for multiple tests ($P \leq 0.01$). Pairwise Φ_{st} values can be found in Table 4. Consistent with these results, values of Jost's D were high ($D > 0.75$) between most collection sites (excluding those in the Atlantic which in which D was effectively zero) except for TW-WAUS ($D = 0.33$). Jost's D values are presented in Table 4.

In the SAMOVA analysis, between group variance was maximized when Atlantic sites were grouped together and all Pacific and Indian Ocean sites were held separately ($\%V = 63.95$, $P = 0.008$). When samples were placed into Atlantic and Indo-Pacific groups, South Africa grouped with the Atlantic samples (SAMOVA groupings in Electronic Appendix C1).

Table 1 Summary statistics for eight microsatellite loci within collections of sandbar shark from Taiwan (TW), Hawaii (HI), eastern Australia (EAUS), western Australia (WAUS), South Africa/Indian Ocean (SAFR), Gulf of Mexico (GOM), Delaware Bay (DEL), Chesapeake Bay (CB) and the lagoons of the Eastern Shore of Virginia (ES)

Sample	Locus Cli12	Cli103	Cpl53	Cpl90	Cpl128	Cpl132	Cpl166	Cpl169
TW								
N	48	48	48	48	48	48	48	48
A	11	15	7	22	29	18	45	31
R	7.713	10.392	5.455	15.355	15.371	12.051	21.02	17.499
Ho	0.77	0.88	0.58	0.98	0.94	0.92	1.00	1.00
He	0.73	0.88	0.70	0.94	0.94	0.90	0.98	0.96
HW	0.7942	0.8733	0.5311	0.6192	0.7393	0.8663	1	0.4152
WAUS								
N	30	30	30	30	30	30	30	30
A	8	15	5	23	16	17	29	25
R	7.203	11.841	4.773	15.899	11.685	12.771	18.884	17.671
Ho	0.73	0.87	0.43	1.00	0.80	0.90	0.93	0.97
He	0.73	0.91	0.69	0.95	0.89	0.91	0.96	0.96
HW	0.5871	0.4341	**0.002**	0.1066	0.0416	0.6932	0.3287	0.6961
HI								
N	23	23	23	23	23	23	23	22
A	3	9	5	10	11	8	23	14
R	2.981	8.059	4.461	8.369	8.598	6.799	16.508	12.206
Ho	0.39	0.87	0.61	0.91	0.65	0.83	0.91	0.95
He	0.40	0.84	0.65	0.75	0.78	0.79	0.94	0.85
HW	0.5689	0.9715	0.9045	0.5278	0.1489	0.7454	0.5945	0.7914
EAUS								
N	43	43	43	43	43	43	43	43
A	22	14	6	24	19	15	42	29
R	7.711	10.623	5.003	14.671	11.93	10.802	21.6	17.992
Ho	0.74	0.88	0.67	1.00	0.81	0.86	0.98	0.95
He	0.65	0.87	0.64	0.94	0.91	0.90	0.98	0.96
HW	0.9092	0.4366	0.8189	0.3539	0.1129	0.2769	0.8022	0.0693
SAFR								
N	15	15	15	15	14	15	14	15
A	9	13	6	17	12	15	18	19
R	8.798	12.655	5.864	16.389	12	14.524	18	17.998
Ho	0.67	1.00	0.67	0.93	0.79	0.87	0.93	0.93
He	0.83	0.91	0.72	0.95	0.92	0.94	0.96	0.94
HW	0.1592	0.9778	0.4156	0.7338	0.1224	0.4595	0.147	0.4105
GOM								
N	23	23	23	23	23	23	23	23
A	10	7	4	17	10	8	24	23
R	9.195	6.108	3.798	14.308	8.777	7.287	18.443	17.25
Ho	0.87	0.70	0.57	0.91	0.78	0.87	0.96	0.91
He	0.88	0.70	0.60	0.93	0.81	0.79	0.97	0.95
HW	0.9452	0.0398	0.6357	0.0931	0.5605	0.9823	0.7528	0.3724
ES								
N	52	52	52	52	52	52	52	52
A	12	8	4	21	15	10	39	34
R	8.413	5.99	3.324	13.263	9.487	7.983	19.979	17.78
Ho	0.90	0.67	0.56	0.92	0.83	0.79	0.98	0.96
He	0.84	0.67	0.58	0.92	0.84	0.83	0.97	0.96
HW	0.6298	0.6752	0.5668	0.2592	0.4022	0.5738	0.4097	0.5389
DEL								
N	55	55	55	55	55	55	55	55
A	10	10	4	20	18	13	47	33
R	7.778	6.315	2.701	12.122	9.79	8.891	20.82	17.096
Ho	0.87	0.73	0.47	0.89	0.85	0.92	1	0.93
He	0.84	0.64	0.54	0.89	0.85	0.85	0.98	0.95

Table 1 (*Continued*)

Sample	Locus Cli12	Cli103	Cpl53	Cpl90	Cpl128	Cpl132	Cpl166	Cpl169
HW	0.0941	0.365	0.7084	0.7667	0.998	0.183	0.9909	0.1878
CB								
N	47	46	46	47	47	47	47	47
A	10	7	3	20	14	10	36	31
R	7.949	5,413	2.773	12.158	9.448	7.855	20.064	16.847
H_O	0.91	0.50	0.50	0.98	0.87	0.87	0.94	0.96
He	0.86	0.50	0.54	0.90	0.87	0.84	0.97	0.95
HW	0.953	0.5597	0.7576	0.5382	0.659	0.5617	0.3896	0.5713

N: number of sharks; *A*: number of alleles; *R*: allelic richness; H_o: observed heterozygosity; H_e: expected heterozygosity; HW: probability of conformance to the expectations of Hardy–Weinberg equilibrium. Bold values indicate significance after correction for multiple tests (initial $\alpha = 0.05$).

Table 2 Summary statistics for mtDNA haplotypes by population and across all populations (Total)

	N	H	s	*h*	π
TW	46	16	9	0.900	0.00211
WAUS	25	13	10	0.930	0.00224
HI	23	4	4	0.542	0.00161
EAUS	43	10	12	0.542	0.00223
SAFR	15	8	17	0.867	0.00468
GOM	23	13	8	0.953	0.00207
ES	52	16	12	0.908	0.00196
DEL	55	18	11	0.909	0.00210
CB	47	22	14	0.932	0.00219
Total	329	67	39	0.959	0.00475

N: number of sharks; *H*: number of haplotypes; *s*: number of variable sites; *h*: nucleon diversity; π: nucleotide diversity.

AMOVA detected significant population structure for microsatellite data, with significant components of variance within and between ocean basins ($\Phi_{SC} = 0.0107$, $\%V = 1.02$, $P < 0.0001$ and $\Phi_{CT} = 0.0498$, $\%V = 44.98$, $P = 0.0049$, Table 3). Pairwise comparisons using microsatellite data showed no significant genetic differentiation between collection sites in the Atlantic Ocean after correction for multiple tests. Atlantic Ocean sites were significantly differentiated from all Pacific and Indian Ocean sites after correction for multiple tests ($P \leq 0.01$). HI was significantly different from all other collection sites after correction for multiple tests ($P \leq 0.01$). WAUS showed significant differentiation from all other collection sites ($P \leq 0.01$), except TW ($F_{ST} = 0.0011$, $P = 0.31$), EAUS ($F_{ST} = 0.0048$ $P = 0.044$) and SAFR ($F_{ST} = 0.010$ $P = 0.044$), but these differences were not significant at the $P \leq 0.05$ level after correction for multiple tests. TW was not significantly differentiated from SAFR ($F_{ST} = -0.0001$, $P = 0.47$) but it was significantly differentiated from EAUS ($F_{ST} = 0.007$, $P = 0.0022$) at the $P \leq 0.05$ but not the $P \leq 0.01$ level. All pairwise F_{ST} values are presented in Table 4. A similar pattern was seen in values of Jost's *D* with relatively high values ($D > 0.15$) between some collection sites, while values were close to zero between TW, WAUS, EAUS and SAFR ($D < 0.053$). In addition, *D* was close to zero between all Atlantic sites ($D < 0.005$). A Mantel test showed that values of Jost's *D* calculated from the different marker types were not significantly correlated ($P = 0.13$).

In the SAMOVA analysis, between group variance was maximized when Atlantic sites were grouped together, EAUS, WAUS, TW and SAFR were grouped together

Table 3 Results of hierarchical AMOVA using mtDNA sequence and microsatellite data

Comparison mtDNA		DF	SSD	VC	%V	Φ	*P*-Value
Among Ocean Basins	FCT	1	289.972	1.7367	56.54	0.5654	0.0075
Among Populations within Oceans	FSC	7	75.334	0.2757	8.98	0.2066	< 0.0001
Within Populations	FST	320	338.89	1.0590	34.48	0.6552	< 0.0001
Microsatellite							
Among Ocean Basins	FCT	1	65.416	0.1763	44.98	0.0498	0.0049
Among Populations within Oceans	FSC	7	41.467	0.0361	1.02	0.0107	< 0.0001
Among Individuls Within Populations	FIS	327	1087.42	−0.0054	−0.15	−0.0016	0.5771
Within Individuals	FIT	336	1121.0	3.3363	94.16	0.0584	< 0.0001

DF: degrees of freedom; SSD: sum of squares; VC: variance component; %*V*: percent of variance.

Table 4 Pairwise Φ_{st} values for mtDNA control region sequence data (above diagonal), pairwise F_{st} values for microsatellite data (below diagonal) and Jost's D for both marker types (in parenthesis) between sandbar shark sample locations

	TW	WAUS	HI	EAUS	SAFR	GOM	ES	DEL	CB
TW	-	**0.1777*** (0.328)	**0.3144*** (0.784)	**0.2881*** (0.948)	**0.6502*** (1.00)	**0.6906*** (1.00)	**0.6766*** (1.00)	**0.6605*** (1.00)	**0.6623*** (1.00)
WAUS	0.00107 (0.000)	-	**0.4104*** (0.964)	**0.1314*** (0.814)	**0.6165*** (1.00)	**0.6746*** (1.00)	**0.6665*** (1.00)	**0.6522*** (1.00)	**0.6490*** (1.00)
HI	**0.0421*** (0.208)	**0.0540*** (0.239)	-	**0.4671*** (1.00)	**0.6657*** (1.00)	**0.6913*** (1.00)	**0.6743*** (1.00)	**0.6593*** (1.00)	**0.6564*** (1.00)
EAUS	**0.0070** (0.001)	0.0048 (0.005)	**0.0624*** (0.289)	-	**0.5880*** (1.00)	**0.6781*** (1.00)	**0.6761*** (1.00)	**0.6571*** (1.00)	**0.6604*** (1.00)
SAFR	−0.0001 (0.006)	0.0101 (0.032)	**0.0562*** (0.242)	**0.0155*** (0.053)	-	**0.4412*** (0.969)	**0.4685*** (0.966)	**0.4284*** (0.947)	**0.4379*** (0.958)
GOM	**0.0428*** (0.208)	**0.0463*** (0.226)	**0.1050*** (0.394)	**0.0477*** (0.197)	**0.0378* (0.150)**	-	−0.0148 (0.000)	0.0181 (0.023)	−0.0092 (0.000)
ES	**0.0438*** (0.231)	**0.0483*** (0.217)	**0.0975*** (0.349)	**0.0551*** (0.241)	**0.0349* (0.149)**	−0.0152 (0.000)	-	0.0052 (0.000)	−0.0164 (0.000)
DEL	**0.0495*** (0.242)	**0.0539*** (0.268)	**0.1076*** (0.422)	**0.0588*** (0.245)	**0.0420* (0.239)**	−0.0003 (0.001)	−0.0014 (0.001)	-	−0.0066 (0.026)
CB	**0.0591*** (0.286)	**0.0632*** (0.253)	**0.1189*** (0.455)	**0.0666*** (0.274)	**0.0520*** (0.270)	0.0039 (0.003)	0.0023 (0.005)	0.0008 (0.002)	-

Values significant at $\alpha = 0.05$ after sequential Bonferroni are bolded. Values significant at $\alpha = 0.01$ after sequential Bonferroni correction denoted by *.

and Hawaii was kept separate (%V = 5.65, P = 0.002, SAMOVA groupings in Appendix B2). Structure analyses detected four populations ($P(k) > 0.99$). In all individual simulations (k = 4) Atlantic sites were grouped together, WAUS and EAUS were grouped together and Hawaii was kept separate. However, TW grouped with SAFR in three simulations and was split between WAUS/EAUS and SAFR in two simulations (Electronic Appendix C). The proportion of membership of TW samples to a given cluster was never greater than 70%.

Correspondence analysis using microsatellite data demonstrated hierarchical population structure. Atlantic Ocean collections grouped together separate from Pacific and Indian Ocean collections (Electronic Appendix D1). When Pacific and Indian Ocean collections were examined separately, HI and SAFR separated from TW, EAUS and WAUS (Fig. 2). When HI and SAFR were excluded TW, EAUS and WAUS were separate but largely overlap (Electronic Appendix D2).

The minimum spanning network based on mitochondrial control region sequences was composed of 44 Steiner trees. There was high support for the majority of connections (Fig. 3). The network indicates two major haplogroups, Pacific and Atlantic. Three SAFR haplotypes were placed between the larger haplogroups, four SAFR haplotypes grouped within the Atlantic haplogroup and the remaining SAFR haplotype grouped with the Pacific haplogroup. HI haplotypes appeared in two separated clusters within the Pacific haplogroup. Haplotypes for the GOM and the three western North Atlantic collection sites were well mixed.

Gene flow

Estimates of M from the Migrate analysis ranged from 0.07 (HI to GOM) to 2.61 (WAUS to EAUS). All but seven estimates of M were less than or not significantly different than one (Table 5). For those estimates of M that were larger than one, migration appeared to be symmetrical (WAUS $\rightarrow$ TW M = 1.76 and TW $\rightarrow$ WAUS M = 1.52; EAUS $\rightarrow$ TW M = 2.11 and TW $\rightarrow$ EAUS M = 2.33; EAUS $\rightarrow$ WAUS M = 1.87 and WAUS $\rightarrow$ EAUS M = 2.61). There were only two cases of asymmetry. The first involved TW and SAFR, where migration to SAFR was negligible (0.41) but migration to TW was significantly greater than one (1.25; C.I. 1.05–1.48). A similar pattern was observed between TW and HI, though gene flow from HI to TW was not significantly greater than one (1.05; C.I. 0.86–1.26).

IMA analysis for most pairwise comparisons produced consistent results among runs when starting points or priors were changed. The exception was the comparison between TW and HI where distributional peaks for the estimated parameters shifted when the priors were changed. The posterior probability did not include zero for either TW_HI or EAUS_HI comparisons (Fig. 4a) using either mtDNA or microsatellites, indicating population divergence based on both marker types. The remaining pairwise comparisons (TW_EAUS, TW_WAUS and EAUS_WAUS) had posterior probabilities of t that peaked at or were very close to zero with high probabilities around zero using microsatellite data, indicating that these molecular markers revealed no divergence (Fig. 4a). For these same comparisons, using mtDNA data, posterior probabilities for t did not include zero (Fig 4a), indicating divergence.

Migration patterns were evaluated for pairwise comparisons between sampling locations using mitochondrial data and between HI and EAUS using microsatellite data, because all showed non-zero divergence. For EAUS_WAUS, the posterior probability of migration in both directions peaked at zero (Fig. 4b), indicating no gene flow since divergence. For TW_EAUS the posterior probability of migration from

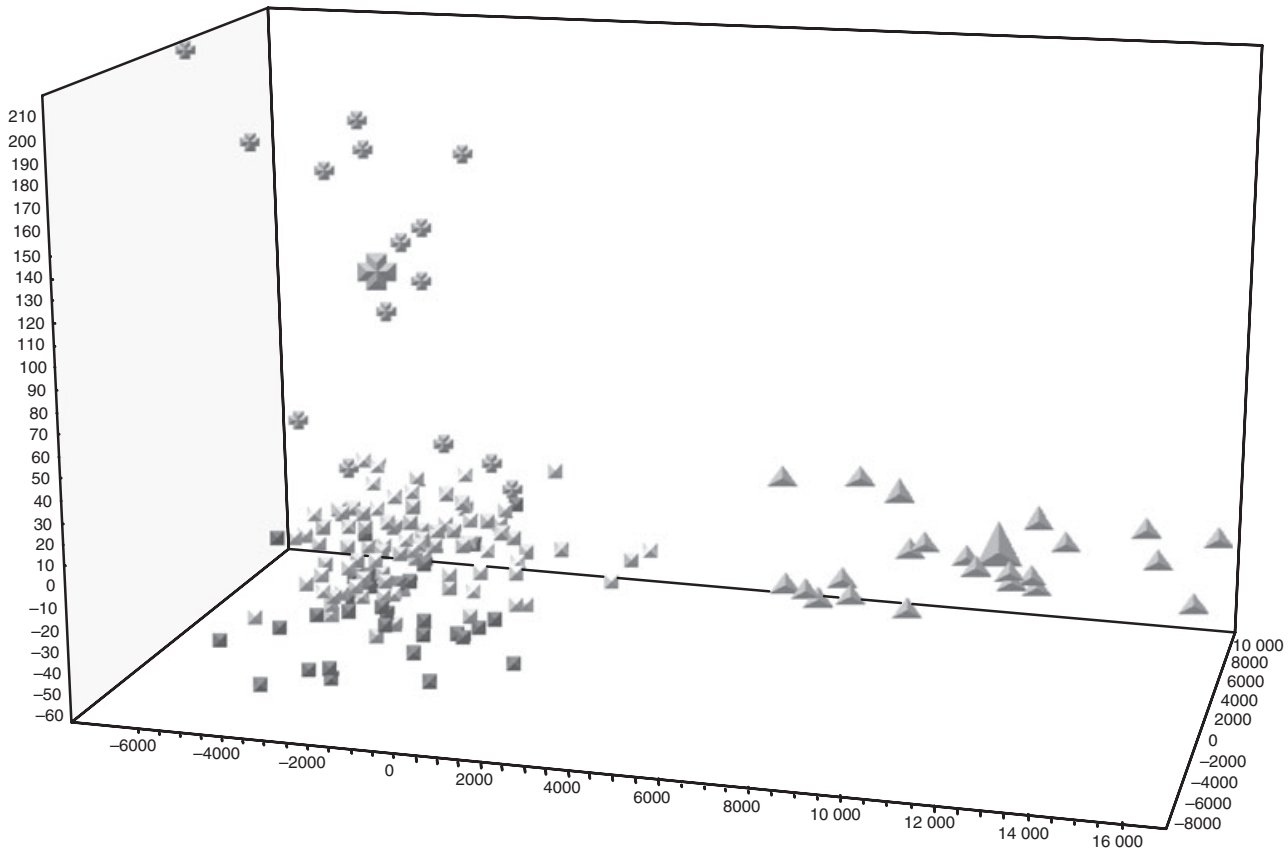

Fig. 2 Correspondence analysis of sandbar shark populations using microsatellite data with Atlantic Ocean samples excluded. Grey crosses are South Africa (SAFR), grey triangles are Hawaii (HI), white squares are eastern Australia (EAUS), dark square are western Australia (WAUS) and lightly shade squares are Taiwan (TW). For SAFR and HI enlarged shape represents population means.

to TW to EAUS peaked at zero. The posterior probability of migration from EAUS to TW peaked close to zero (0.075) but the peak probability was more than three times the probability at zero (Fig 4b). Likelihood ratio tests rejected a null model of zero gene flow (2LLR = 6.81, $P = 0.03$, df = 2) but could not reject a null model with zero gene flow from TW to EAUS and non-zero gene flow from EAUS to TW (2LLR = 0.15, $P = 0.70$, df = 1). For TW_WAUS data both distributions peaked further from zero ($m_{1(\text{WAUS to TW})} = 0.695$, $m_{2(\text{TW to WAUS})} = 0.255$; Fig 4b), but peak probabilities were similar to the probability of zero. Likelihood ratio tests rejected a null model of zero gene flow (2LLR = 9.08, $P = 0.007$, df = 2) and a null model with zero gene flow from WAUS to TW and non-zero gene flow from TW to WAUS (2LLR = 4.16, $P = 0.041$, df = 1). However, a null model of zero gene flow from TW to WAUS and non-zero gene flow from WAUS to TW could not be rejected (2LLR = 0.001, $P = 0.97$, df = 1). For the EAUS_HI comparison using mtDNA, the distributions of m peaked at or near zero (Fig 4b). A likelihood ratio test could not reject a null model of zero gene flow (2LLR = 2.92, $P = 0.23$, df = 2). For the EAUS_HI comparison using microsatellite data, the posterior probability of migration from HI to EAUS peaked at zero. The posterior probability of migration from EAUS to HI peaked further from zero ($m_2 = 0.495$, Fig. 4b) and the peak probability was 2.5 times the probability at zero. Migration between HI and TW was not evaluated as the distributions were strongly dependent on the priors.

For the three estimates of m that were indicative of gene flow (mtDNA; WAUS → TW and EAUS → TW, microsatellites; EAUS → HI), the posterior distribution of migration events over time were recorded. In all three cases, distributions were tight and the peak probabilities were more recent than the peak probabilities of divergence (Fig. 4c), indicating secondary contact after divergence was likely discrete in time rather than continuous. For two of the comparisons (EAUS → HI and WAUS → TW) gene flow was historical as indicated by distributions with extremely low probabilities at time zero. On the other hand, gene flow from EAUS to TW (mtDNA data) appears to be contemporary or in the recent past as the distribution peaks at time zero.

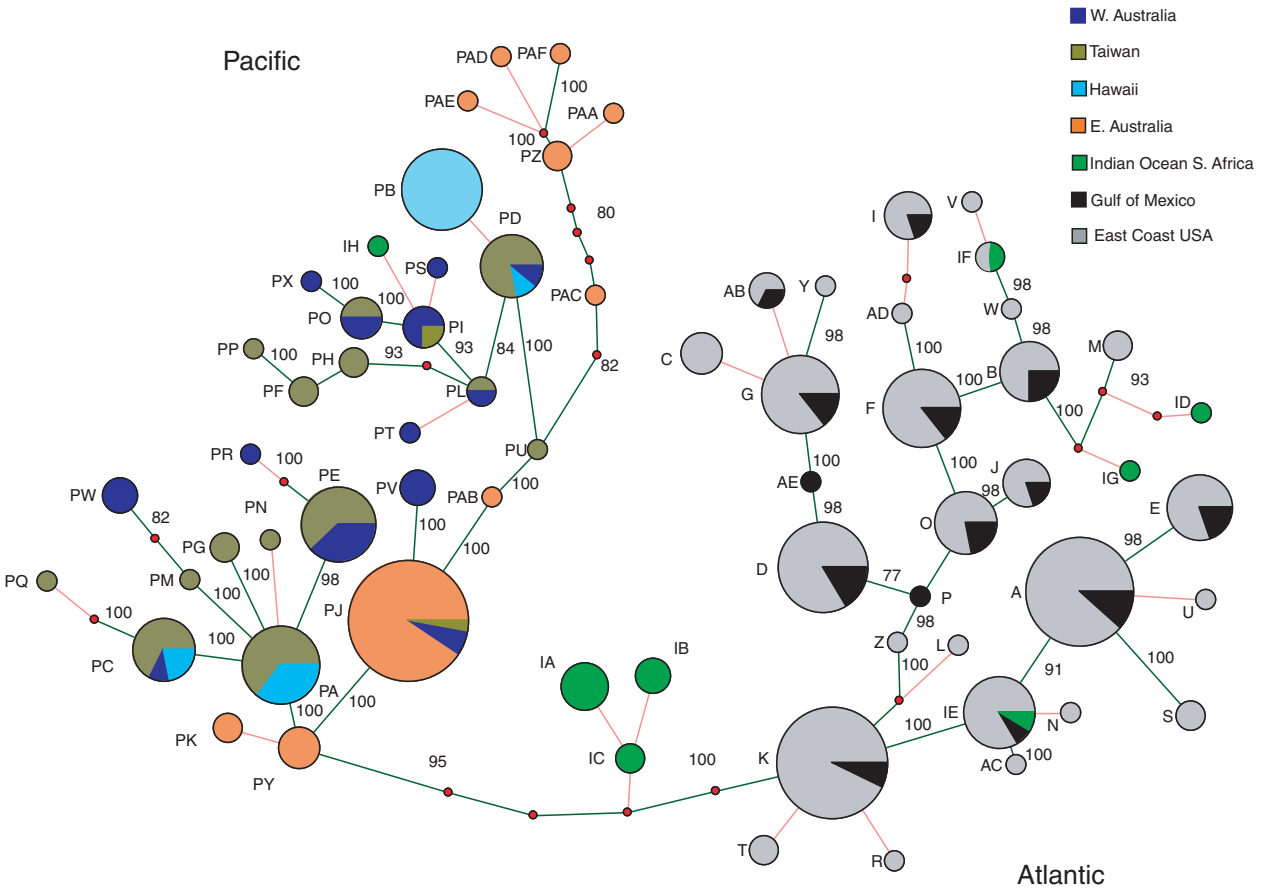

Fig. 3 Minimum spanning network of 67 sandbar shark haplotypes found in this study created using the median joining algorithm. Support values (% of Steiner trees with connection) are listed to the right or above connections. Connections in torso are green, connection exterior to torso are red.

Table 5 Values of M (mutational corrected migration) generated in MIGRATE analysis from microsatellite data between populations, defined by analysis of mtDNA sequences

I	TW	WAUS	HI	EAUS	SAFR	GOM
TW	-	**1.52 (1.29–1.75)**	0.47 (0.36–0.61)	**2.33 (2.06–2.63)**	0.41 (0.31–0.52)	0.57 (0.44–0.72)
WAUS	**1.76 (1.52–2.03)**	-	0.42 (0.30–0.55)	**2.61 (2.32–2.93)**	0.34 (0.25–0.45)	0.21 (0.14–0.31)
HI	1.05 (0.86–1.26)	0.09 (0.04–0.15)	-	0.73 (0.58–0.90)	0.14 (0.11–0.19)	0.07 (0.04–0.14)
EAUS	**2.11 (1.84–2.40)**	**1.87 (1.64–2.14)**	0.59 (0.46–0.75)	-	0.45 (0.35–0.57)	0.47 (0.35–0.61)
SAFR	**1.25 (1.05–1.48)**	0.71 (0.58–0.87)	0.16 (0.09–0.23)	0.39 (0.28–0.51)	-	0.19 (0.12–0.28)
GOM	0.48 (0.36–0.62)	0.24 (0.17–0.34)	0.08 (0.04–0.14)	0.20 (0.13–0.30)	0.32 (0.24–0.42)	-

Donor populations are on vertical, recipient populations are on the horizontal. 95% CI are in parenthesis. M values significantly greater than 1 are in bold.

Discussion

Population structure and contemporary gene flow

In this study we attempted to examine patterns of population structure and gene flow on a global scale. While sampling was widespread, covering the species' cosmopolitan range, it was not complete. Within the Atlantic Ocean, samples came from a limited region in the western North Atlantic. These samples show no signs of divergence using data from either mtDNA sequences or microsatellites. This confirms earlier work using allozymes and mtDNA RFLPs, which suggested that the Gulf of Mexico and western North Atlantic

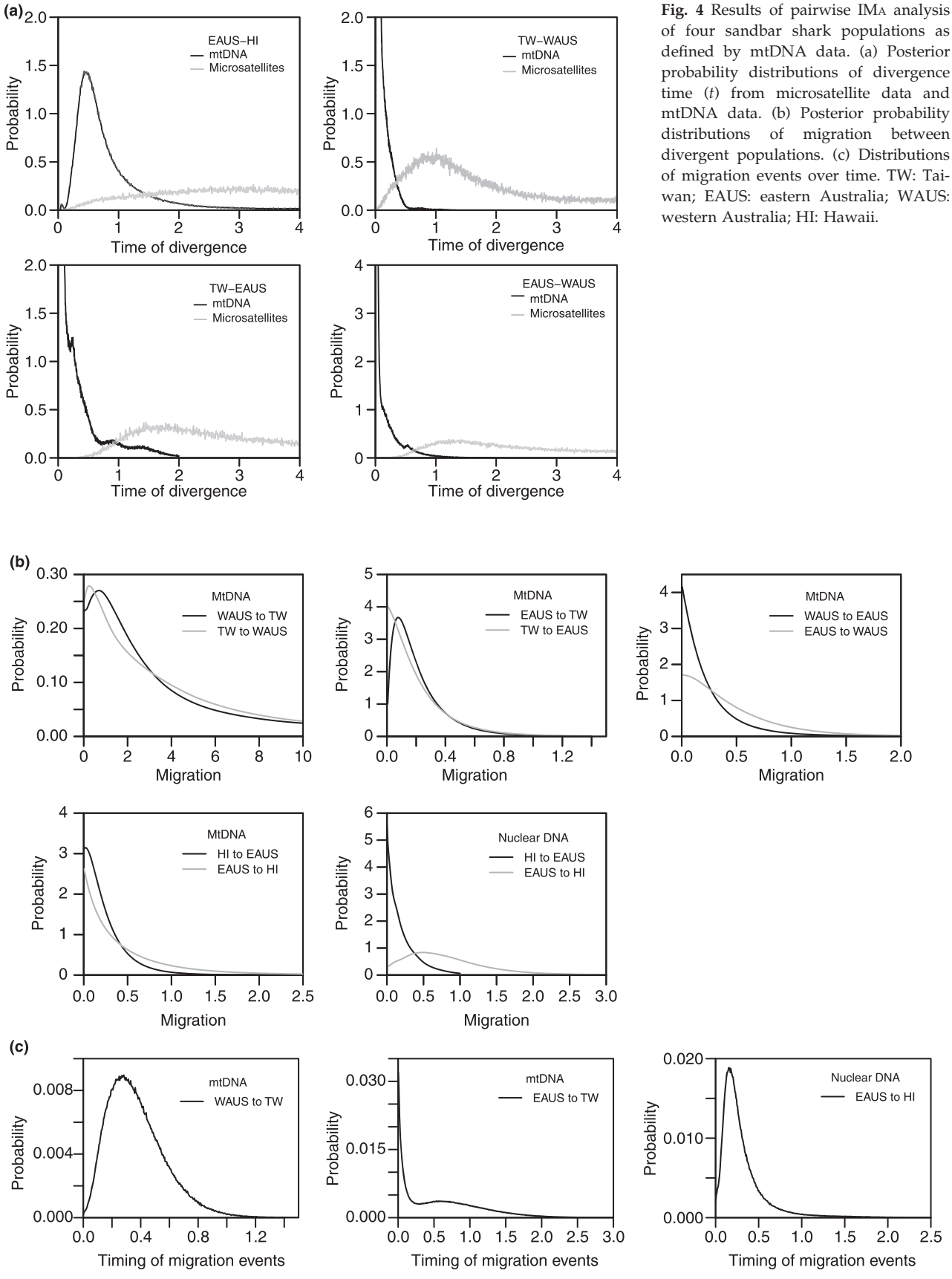

Fig. 4 Results of pairwise IMA analysis of four sandbar shark populations as defined by mtDNA data. (a) Posterior probability distributions of divergence time (*t*) from microsatellite data and mtDNA data. (b) Posterior probability distributions of migration between divergent populations. (c) Distributions of migration events over time. TW: Taiwan; EAUS: eastern Australia; WAUS: western Australia; HI: Hawaii.

were part of one panmictic unit (Heist *et al.* 1995). Thus only one Atlantic Ocean population was sampled.

Two mitochondrial haplotypes were shared between the western North Atlantic and the western Indian Ocean. This could be the result of contemporary gene flow around the tip of Africa, a phenomenon seen in other marine species such as the escolar, *Lepidocybium flavobrunnem* (Brendtro *et al.* 2008). Alternatively, as many marine species seem to have dispersed around the tip of Africa historically (Goodbred & Graves 1996; Scoles *et al.* 1998; Bowen *et al.* 2006), it could reflect incomplete lineage sorting resulting from a recent, shared ancestral gene pool. If the observed shared haplotypes are indeed the result of contemporary gene flow, it would seem to be going from the Atlantic to the Indian Ocean, a phenomenon observed in other highly migratory species like green turtles and scalloped hammerhead sharks (Duncan *et al.* 2006; Bourjea *et al.* 2007). In addition, dispersal from the Indian Ocean could have originally been to the western South Atlantic, rather than the eastern Atlantic, with a subsequent dispersal throughout the rest of the Atlantic, as is suggested for a variety of marine species (molluscs—Vermeij & Rosenberg 1993; turtles—Bowen *et al.* 1994; fish—Rocha *et al.* 2005). Without samples from the eastern Atlantic and western South Atlantic, these hypotheses cannot be tested for the sandbar shark.

Sampling was more complete in the central Indo-West Pacific and sample sizes per location were larger. All pairwise comparisons between central Indo-West Pacific collections exhibited large and significant Φ_{ST} values and correspondingly large Jost's *D* values, indicating a cessation of contemporary female gene flow. However, small non-significant pairwise microsatellite F_{ST} values and correspondingly small Jost's *D* values between WAUS and TW as well as EAUS and WAUS indicate there may be contemporary, male-mediated gene flow. This conclusion is further supported by the fact that divergence was not correlated across marker type, suggesting different genealogical/demographic histories.

Analyses using the SAMOVA and Structure software packages also show discordance between marker types, recovering the same basic groupings as pairwise F_{ST} analysis. In addition, the result of the Migrate analysis using microsatellite data detected much higher levels of mutation scaled migration between TW, WAUS and EAUS than between any other locations. Finally, the results of the IMA analysis using microsatellite data detected zero divergence between these locations, likely indicating high levels of contemporary or relatively recent gene flow. On the other hand, the same analysis using mtDNA data showed divergence with either zero or restricted gene flow.

Pairwise F_{ST} values were also small and non-significant between SAFR and TW and SAFR and WAUS, with correspondingly small Jost's D values, indicating that there may also be male-mediated gene flow between these regions. The SAMOVA analysis supported this supposition by grouping TW, SAFR, WAUS and EAUS while the Structure analysis placed TW and SAFR together and often separate from WAUS and EAUS. The results of the Migrate analysis also support the possibility of gene flow from SAFR to TW. However, the perceived relationship between TW and SAFR may be due in part to the limited power of these analyses resulting from the small size of the SAFR sample (15). The pairwise F_{ST} value between WAUS and SAFR is non-significant after correction but is larger at 0.01006 ($P = 0.047$) than other F_{ST} values found to be significant (EAUS-TW $F_{ST} = 0.0073$, $P = 0.0021$). Correspondence analysis supports the notion that the grouping of SAFR with WAUS and TW may be influenced by small sample size as it shows SAFR as distinct from TW and WAUS. If there is male-mediated gene flow, the conclusion would be aided by augmenting the SAFR samples to look for gene flow between SAFR and a geographically more proximate population. Given the geographical distance, it seems that direct contemporary gene flow between SAFR and the central Indo-West Pacific is unlikely.

The presence of contemporary male-mediated gene flow is further supported by the signature of past secondary contact between EAUS and HI, which is evident in the microsatellite data but not in the mtDNA data. These findings are similar to those of studies in the western North Atlantic and Gulf of Mexico, which have demonstrated male-mediated gene flow and regional female philopatry in blacktip and lemon sharks (Keeney *et al.* 2005; Schultz *et al.* 2008). Similar patterns suggestive of philopatry and male-mediated gene flow have also been observed across single ocean basins in both white sharks and mako sharks (Pardini *et al.* 2001; Schrey & Heist 2003), while whale sharks may show female philopatry to ocean basins (Castro *et al.* 2007; Schmidt *et al.* 2009).

Historical dispersal

Dispersal between the Pacific and Atlantic Ocean likely occurred via the Indian Ocean. This is supported by the central position of several Indian Ocean haplotypes in the network. The alternative pathway through the eastern Pacific seems unlikely, especially in light of the species' absence from that region. In addition, mtDNA haplotypes found in HI consistently appear distant from the Atlantic haplogroup, while EAUS haplotypes are the most interior Pacific haplotypes in close proxim-

ity to SAFR haplotypes. In addition, multiple SAFR haplotypes are found within the Atlantic group. This suggests a common central Indo-West Pacific origin of EAUS, SAFR and Atlantic Ocean haplotypes, a pattern seen in other shark species including hammerhead and blacktip sharks (Duncan *et al.*2006; Keeney & Heist 2006), as well as in pelagic bony fishes such as sailfish, blue marlin, and bigeye tuna (Graves & McDowell 2003; Martinez *et al.* 2006). However, an Atlantic Ocean origin followed by dispersal through the Indian Ocean cannot be rejected. Either way, the close relationships between the haplotypes suggest that dispersal and subsequent divergence may have been recent.

An important finding of this study was that mitochondrial and nuclear inference placed the Indian Ocean samples within different groups. The former places SAFR closest to Atlantic Ocean samples, while the latter places SAFR with the Pacific Ocean. This suggests that long after female philopatry allowed western Indian Ocean mtDNA haplotypes to diverge from central Indo-West Pacific haplotypes, there may have been male-mediated gene flow from the Pacific. Alternately, since one SAFR mtDNA haplotype is in the Pacific clade, all western Indian Ocean mtDNA haplotypes may originally have been of Pacific origin and were replaced subsequently by Atlantic haplotypes.

The idea that male-mediated gene flow could change the nuclear composition of populations is supported by other data in this study. EAUS has the lowest nucleon diversity seen in this study (along with HI), but fairly high allelic richness, a pattern likely created by contemporary male-mediated gene flow from the genetically diverse WAUS and TW into a population founded by a small number of females. This pattern mirrors that seen in bluefish distributed on both coasts of Australia (Goodbred & Graves 1996). In addition, EAUS appears to have had a period of re-established male-mediated gene flow with HI long after divergence. Such a dynamic may explain the patterns seen in SAFR.

There is also evidence to support the idea that secondary female contact may be responsible for the current mtDNA composition of Hawaiian populations. In HI there are groups of divergent mtDNA haplotypes which, when combined with low haplotype diversity, suggest that HI may have been founded by small numbers of females (Avise *et al.* 1987). This hypothesis is supported by the results of the IMA analysis and the minimum spanning network, which collectively suggest that HI haplotypes may have originated from events separated in time and space. Such a scenario has previously been suggested as an explanation for divergent mtDNA lineages in Atlantic blue marlin, Atlantic sailfish and spotted chub mackerel that have been found to co-occur in certain geographic locations (Graves 1998). However, HI has seemingly been isolated for some time, as it appears very divergent from other sampling locations regardless of marker type. Consistent with this scenario, the life history characteristics of the sandbar sharks in HI are also divergent from other populations. In HI sandbar sharks mature at smaller sizes, have smaller litters and have different behaviour, such as using the deep slope for nurseries instead of embayments and estuaries (Romine *et al.* 2006).

Migrate and IMA analyses also suggest that TW has received pulses of male and female migrants. While contemporary male-mediated gene flow was detected between TW, WAUS and EAUS there also appear to be small amounts of recent female migration from EAUS to TW and in the more distant past from WAUS to TW. The two migration asymmetries detected with Migrate also suggest gene flow toward TW.

Overall, these data present evidence for a complex history featuring divergence and pulses of secondary contact, often followed by a further period of isolation. For TW in particular, it appears that the result may be a mixing of genetic material from a number of different source populations. This may in part explain some of the difficulties in modelling the relationship between HI and TW with IMA.

To understand the environmental processes responsible for the observed patterns of divergence and secondary contact, it is desirable to approximate divergence times from the IMA estimates of t. However, given the uncertainty about microsatellite mutation rates in elasmobranchs, the calculations would be subject to considerable error. There are, however, more reliable estimates for the mtDNA control region divergence rate for carcharinid species (0.43%MY—Keeney & Heist 2006; 0.8%/MY—Duncan *et al.* 2006; 0.6%/MY—Schultz *et al.* 2008). Using the extreme values, we calculated the actual divergence time for the largest point estimate of $t = 3.23$ based on mtDNA, which comes from the EAUS_HI comparison. This results in an estimate of divergence between 403 750–751 162 years ago, well within the Pleistocene which began 2 million years ago. For the other mtDNA-based estimates of t, which varied from 1.45 to 1.01, the estimated divergence times would be between 181 250–337 209 and 126 250–234 883 years ago, respectively. The pooled Atlantic and Pacific data produced estimates of $t = 1.995$, placing the split between these distinct phylogroups 249 375–463 953 years ago, after the split between EAUS and HI but before the WAUS, TW and EAUS diverged. The only microsatellite based estimate of t (0.429; EAUS_HI) had tight confidence intervals (0.15–1.81). For t to fall before the Pleistocene would require a mutation rate between 1.5×10^{-6} and 1.8×10^{-5} mutations per locus per generation, and this would be

amongst the slowest reported microsatellite mutation rates (Hancock 1999).

Given these calculations, it seems reasonable to suggest the events responsible for the current patterns of genetic divergence in sandbar sharks occurred largely within the last 2 million years. During this time, there were as many as 20 glacial periods, each lasting approximately 100 000 years, followed by shorter interglacial periods of about 10 000 years (Martinson *et al.* 1987; Dawson 1992). As glacial extent fluctuated, so did the latitudinal extent of tropical and subtropical waters (Savin *et al.* 1975). During the long periods of glaciations, temperature may have restricted the sandbar sharks' range, while during shorter interglacial periods; increased temperature at higher latitudes may have allowed pulses of dispersals. This pattern of pulses of range expansion coinciding with periods of glacial lows, followed by isolation during periods of glacial highs has been demonstrated in other fishes and marine mammals (Johnson 2003; Harlin-Cognato *et al.* 2006).

Unlike these studies which demonstrated pulses of isolation and range expansion, the data in this study also show a pattern of persisting male gene flow after the cessation of female gene flow. Since temperature constraints are likely to be a function of the basic biology of the animal, changing temperatures would most likely affect sex specific dispersal potential equally. Perhaps a more important factor is that during glacial periods, sea level was as much as 100 m lower than today (Shackleton 1987). This may have created barriers which isolated formerly connected populations and changed the distribution of the shallow near-shore habitats that most sandbar shark populations use as nurseries. As an example, falling sea levels during glacial maxima increased dry land in the Indonesian archipelago (Heaney 1991), perhaps making migration from tropical WAUS to the Pacific more difficult. At the same time, estuaries and shallow coastal environments that that currently serve as sandbar shark nurseries (Castro 1993; Joung & Chen 1995) off the east coast of Asia and North America would have been dry land, only flooding after about 12 000 ybp (Kraft 1977; Verstappen 1980). In areas where appropriate nursery grounds disappeared and/or temperature decreased, populations might have dwindled only to be resurrected by migrants from other locations when appropriate conditions returned. This type of dynamic may explain the recurring pattern of gene flow towards TW seen in this study.

For females, an increase in the number of appropriate nursery areas following climate change, especially in the periphery of the species' range, might allow for straying and a gradual range expansion. Such straying has been suggested as an explanation for the colonization of new nesting beaches in sea turtles, which show strong philopatric behaviour (Bowen *et al.* 1992). During the following climate shift, these nurseries might drain, effectively halting female dispersal and perhaps dividing formerly continuous distributions. However, if the temperature between these discontinuous groups was appropriate, male-mediated gene flow may have continued.

Conclusion

This study demonstrates different patterns of contemporary gene flow and historical dispersal using markers with different modes of inheritance. Analysis indicates the distribution of sandbar sharks may have been influenced by differences in patterns of male and female dispersal. Analysis of nuclear markers indicates that on contemporary time scales, male-mediated gene flow exists over long distances and that there is often a cessation of female gene flow prior to a cessation of male gene flow. A number of prior studies have detected population structure in elasmobranchs using only mtDNA. Since males of many other species have great dispersal potential it will be important to reassess the conclusions of these studies using nuclear markers especially as they apply to the definition of stock structure.

Acknowledgements

The authors wish to thank Christina Conrath, J. Spencer Smith, Jason Romine, R. Dean Grubbs, Chip Cotton, W. David McElroy, Naeem Willet, Dr. Shoou-Jeng Joung, Sabine Winter and Lenore Litherland for assistance in collecting specimens. We would also like to thank Sean Rogers and six anonymous reviewers for their helpful comments and suggestions. A portion of the funding for this project came from the National Marine Fisheries Service's Highly Migratory Species Division through the Virginia Institute of Marine Science, a member institute in the National Shark Research Consortium. Part of this work was carried out by using the resources of the Computational Biology Service Unit from Cornell University which is partially funded by Microsoft Corporation. This is VIMS contribution 3072.

References

Avise JC (1998) Conservation genetics in the marine realm. *The Journal of Heredity*, **89**, 377–382.

Avise JC (2000) *Phylogeography: the History and Formation of Species*. Harvard University Press, Cambridge, MA.

Avise JC, Arnold J, Ball RM *et al.* (1987) Intraspecific phylogeography: the mitochondrial DNA bridge between population genetics and systematics. *Annual Review in Ecology and Systematics*, **18**, 489–522.

Bandelt H, Forster P, Rohl A (1999) Median-joining networks for inferring intraspecific phylogenies. *Molecular Biology and Evolution*, **16**, 37–48.

Beerli P, Felsenstein J (1999) Maximum-likelihood estimation of migration rates and effective population numbers in two populations using a coalescent approach. *Genetics*, **152**, 763–773.

Belkhir K, Borsa P, Chikhi L, Raufaste N, Bonhomme F (2004) *Genetix, logiciel sous Windows TM pour la genetique des populations*. Laboratoire Genome Populations, Montpellier, France, Interactions CBRS UMR 5000.

Bourjea J, Lapegue S, Gagnevin L *et al.* (2007) Phylogeography of the green turtle, *Chelonia mydas*, in the Southwest Indian Ocean. *Molecular Ecology*, **16**, 175–186.

Bowen BW, Meylan A, Ross J *et al.* (1992) Global population structure and natural history of the green turtle (*Chelonia mydas*) in terms of matriarchal phylogeny. *Evolution*, **46**, 865–881.

Bowen BW, Kamezaki N, Limpus CJ *et al.* (1994) Global phylogeography of the loggerhead turtle (*Caretta caretta*) as indicated by mitochondrial DNA haplotypes. *Evolution*, **48**, 1820–1828.

Bowen BW, Muss A, Rocha LA, Grant WS (2006) Shallow mtDNA coalescence in Atlantic pygmy angelfishes (Genus *Centropyge*) indicates a recent invasion from the Indian Ocean. *Journal of Heredity*, **97**, 1–12.

Branstetter S (1990) Early life-history implications of selected carcharhinoid and lamnoid sharks of the Northwest Atlantic. In: *Elasmobranchs as Living Resources; Advances in the Biology, Ecology, Systematics and the Status of the Fisheries* (eds Pratt HL, Gruber SH, Taniuchi T), pp. 17–28. NOAA NMFS Technical Report 90.

Brendtro K, McDowell JR, Graves JE (2008) Population genetic structure of escolar (*Lepidocybium flavobrunnem*). *Marine Biology*, **155**, 11–22.

Buonaccorsi VP, McDowell JR, Graves JE (2001) Reconciling patterns of inter-ocean molecular variance from four classes of molecular markers in blue marlin (*Makaira nigicans*). *Molecular Ecology*, **10**, 1179–1196.

Castro JI (1993) The shark nursery of Bulls Bay, South Carolina, with a review of the shark nurseries of the southeastern coast of the United States. *Environmental Biology of Fishes*, **38**, 37–48.

Castro ALF, Stewart BS, Wilson SG *et al.* (2007) Population genetic structure of the Earth's largest fish, the whale shark (*Rhincodon typus*). *Molecular Ecology*, **16**, 5183–5192.

Chapman DD, Babcock EA, Gruber SH *et al.* (2009) Long-term natal site-fidelity by immature lemon sharks (*Negaprion brevirostris*) at a subtropical island. *Molecular Ecology*, **18**, 3500–3507.

Compagno L, Dando M, Fowler S (2005) *Sharks of the World*. Princeton University Press, Princeton, NJ.

Crawford NG (2009) SMOGD: software for the measurement of genetic diversity. *Molecular Ecology Resources*, **10**, 556–557.

Dawson A (1992) *Ice Age Earth*. Routledge Press, London, 293 pp.

Duncan KM, Martin AP, Bowen BW, de Couet HG (2006) Global phylogeography of the scalloped hammerhead shark (*Sphyrna lewini*). *Molecular Ecology*, **15**, 2239–2251.

Dupanloup I, Schneider S, Excoffier L (2002) A simulated annealing approach to define the genetic structure of populations. *Molecular Ecology*, **11**, 2571–2581.

Estoup A, Largiader CR, Perrot E, Chourrout D (1996) Rapid one-tube DNA extraction for reliable PCR detection of fish polymorphic markers and transgenes. *Molecular Marine Biology and Biotechnology*, **5**, 295–298.

Excoffier L, Smouse PE, Quattro JM (1992) Analysis of molecular variance inferred from metric distances among DNA haplotypes: application to human mitochondrial DNA restriction data. *Genetics*, **131**, 479–491.

Excoffier L, Laval G, Schneider S (2005) ARLEQUIN (version 3.0): an integrated software package for population genetics data analysis. *Evolutionary Bioinformatics Online*, **1**, 47–50.

Falush D, Stephens M, Pritchard JK (2007) Inference of population structure using multilocus genotype data: dominant markers and null alleles. *Molecular Ecology Notes*, **7**, 574–578.

Feldheim KA, Gruber SH, Ashley MV (2002) The breeding biology of lemon sharks at a tropical nursery lagoon. *Proceedings of the Royal Society of London Series B: Biological Sciences*, **269**, 1655–1611.

Goodbred CO, Graves JE (1996) Genetic relationship among geographically isolated populations of bluefish (*Pomatomus saltatrix*). *Marine and Freshwater Research*, **47**, 347–355.

Goudet J (2001) FSTAT, a program to estimate and test gene diversities and fixation indices (Version 2.9.3). Available from http ://http://www.unil.ch/izea/softwares /fstat.html. Updated from Goudet (1995).

Graves JE (1998) Molecular insights into the population structures of cosmopolitan marine fishes. *Journal of Heredity*, **89**, 427–437.

Graves JE, McDowell JR. (2003) Stock structure of the world's istiophorid billfishes: a genetic perspective. *Marine and Freshwater Research*, **54**, 287–298.

Guinand B (1996) Use of a multivariate model using allele frequency distributions to analyze patterns of genetic differentiation among populations. *Biological Journal of the Linnean Society*, **58**, 173–195.

Hancock J (1999) Microsatellites and other simple sequences: genomic context and mutatiomal mechanisms. In:*Microsatellies: Evolution and Application* (eds Goldstein DB, Schlotterer C). pp. 1–6, Oxford Unversity Press, New York.

Harlin-Cognato A, Bickham JW, Loughlin TR, Honeycutt RL (2006) Glacial refugia and the phylogeography of Steller's sea lion (*Eumatopias jubatus*) in the North Pacific. *Journal of Evolutionary Biology*, **19**, 955–969.

Heaney L (1991) A synopsis of climatic and vegetational change in Southeast Asia. *Climatic Change*, **19**, 53–61.

Hedrick PW (1999) Perspective: highly variable loci and their interpretation in evolution and conservation. *Evolution*, **53**, 313–318.

Heist EJ, Graves JE, Musick JA (1995) Population genetics of the sandbar shark (*Carcharhinus plumbeus*) in the Gulf of Mexico and Mid-Atlantic Bight. *Copeia*, **1995**, 555–562.

Hey J, Nielsen EE (2007) Integration within the Felsenstein equation for improved Markov chain Monte Carlo methods in population genetics. *Proceedings of the National Academy of Sciences, USA*, **104**, 2785–2790.

Johnson KR (2003) *A genetic analyses of the intraspecific relationships of tropical marine shorefishes common to Bermuda and the southeastern Atlantic Coast of the United States*, Masters Thesis. Fisheries Science Department, School of Marine Science, The College of William and Mary, Gloucester Point, VA.

Jost L (2008) G_{ST} and its relatives do not measure differentiation. *Molecular Ecology*, **17**, 4015–4026.

Joung SJ, Chen CT (1995) Reproduction in the sandbar shark, *Carcharhinus plumbeus*, in the waters off northeastern Taiwan. *Copeia*, **1995**, 659–665.

Karl SA, Bowen BW, Avise JC (1992) Global population genetic structure and male-mediated gene flow in the green turtle (*Chelonia mydas*): RFLP analyses of anonymous nuclear loci. *Genetics*, **131**, 163–173.

Keeney DB, Heist EJ (2003) Characterization of microsatellite loci isolated from the blacktip shark and their utility in requiem and hammerhead sharks. *Molecular Ecology Notes*, **3**, 501–504.

Keeney DB, Heist EJ (2006) Worldwide phylogeography of the blacktip shark (*Carcharhinus limbatus*) inferred from mitochondrial DNA reveals isolation of western Atlantic populations coupled with recent Pacific dispersal. *Molecular Ecology*, **15**, 3669–3679.

Keeney DB, Heupel M, Hueter RE, Heist E J (2003) Genetic heterogeneity among blacktip shark, *Carcharhinus limbatus*, continental nurseries along the U.S. Atlantic and Gulf of Mexico. *Marine Biology*, **143**, 1039–1046.

Keeney DB, Heupel M, Hueter RE, Heist EJ (2005) Microsatellite and mitochondrial DNA analyses of the genetic structure of blacktip shark (*Carcharhinus limbatus*) nurseries in the Northwestern Atlantic, Gulf of Mexico, and Caribbean Sea. *Molecular Ecology*, **14**, 1911–1923.

Kohler N, Turner PA (2001) Shark tagging: a review of conventional methods and studies. *Environmental Biology of Fishes*, **60**, 191–223.

Kraft JC (1977) Late Quaternary paleogeographic changes in the coastal environments of Delaware, Middle Atlantic Bight, related to archaeological settings. *Annals of the New York Academy of Sciences*, **288**, 35–69.

Machado C, Kliman RM, Markert JM, Hey J (2002) Inferring the history of speciation from multilocus DNA sequence data: the case of *Drosophila pseudoobscura* and its close relatives. *Molecular Ecology*, **19**, 472–488.

Martinez P, Gonzalez EG, Castilho R, Zardoya R (2006) Genetic diversity and historical demography of Atlantic bigeye tuna (*Thunnus obesus*). *Molecular Phylogenetics and Evolution*, **39**, 404–416.

Martinson D, Pisias NG, Hays JD *et al.* (1987) Age, dating and orbital theory of the ice ages: Development of a high resolution 0-300,000 year chronostratigraphy. *Quaternary Research*, **27**, 1–29.

McAuley RB, Simpfendorfer CA, Hyndes GA, Lenanton RCJ (2007) Distribution and reproductive biology of the sandbar shark, *Carcharhinus plumbeus* (Nardo), in Western Australian waters. *Marine and Freshwater Research*, **58**, 116–126.

Niemiller ML, Fitzpatrick BM, Miller BT (2008) Recent divergence-with-gene-flow in Tennessee cave salamanders (Plethodontidae: *Gyrinophilus*) inferred from gene genealogies. *Molecular Ecology*, **17**, 2258–2275.

NOAA (2008) Atlantic highly migratory species; Atlantic commercial shark management measures. *Federal Register, Proposed Rules*, **73**, 63668–63672.

Palumbi SR, Baker CS (1994) Contrasting population structure from nuclear intron sequences and mtDNA of humpback whales. *Molecular Biology and Evolution*, **11**, 426–435.

Palumbi SR, Grabowsky G, Duda T, Geyer L, Tachino N (1997) Speciation and population genetic structure in tropical Pacific sea urchins. *Evolution*, **51**, 1506–1517.

Pardini AT, Jones CS, Noble LR *et al.* (2001) Sex-biased dispersal of great white sharks. *Nature*, **412**, 139–140.

Polzin T, Daneshmand SV (2003) On Steiner trees and minimum spanning trees in hypergraphs. *Operations Research Letters*, **31**, 12–20.

Portnoy DS, McDowell JR, Thompson K, Musick JA, Graves JE (2006) Isolation and characterization of five dinucleotide microsatellite loci in the sandbar shark, *Carcharhinus plumbeus*. *Molecular Ecology Notes*, **6**, 431–433.

Portnoy DS, Piercy AN, Musick JA, Burgess GH, Graves JE (2007) Genetic polyandry and sexual conflict in the sandbar shark, *Carcharhinus plumbeus*, in the western North Atlantic and Gulf of Mexico. *Molecular Ecology*, **16**, 187–197.

Pratt HL, Carrier JC (2001) A review of elasmobranch reproductive behaviour with a case study on the nurse shark, *Ginglymostoma cirratum*. *Environmental Biology of Fishes*, **60**, 157–188.

Raymond M, Rousset F (1995) GENEPOP (version 1.2): population genetics software for exact tests and ecumenicism. *Heredity*, **86**, 248–249.

Rice WR (1989) Analyzing tables of statistical tests. *Evolution*, **43**, 223–225.

Rocha LA, Robertson DR, Rocha CR *et al.* (2005) Recent invasion of the tropical Atlantic by an Indo-Pacific coral reef fish. *Molecular Ecology*, **14**, 3921–3928.

Romine J, Grubbs RD, Musick JA (2006) Age and growth of the sandbar shark, *Carcharhinus plumbeus*, in Hawaiian waters through vertebral analysis. *Environmental Biology of Fishes*, **77**, 229–239.

Rousset F (2008) genepop™ 007: a complete re-implementation of the genepop software for Windows and Linux. *Molecular Ecology Resources*, **8**, 103–106.

Savin SM, Douglas RG, Stehli FG (1975) Tertiary marine paleotemperatures. *The Geological Society of America Bulletin*, **86**, 1499–1510.

Schmidt JV, Schmidt CL, Ozer F *et al.* (2009) Low genetic differentiation across three major ocean populations of the whale shark, *Rhincodon typus*. *PLoS ONE*, **4**, e4988.

Schrey AW, Heist EJ (2003) Microsatellite analysis of population structure in the shortfin mako (*Isurus oxyrinchus*). *Canadian Journal of Fisheries and Aquatic Science*, **60**, 670–675.

Schultz JK, Feldehim K, Gruber SH *et al.* (2008) Global phylogeography and seascape genetics of the lemon sharks (genus *Negaprion*). *Molecular Ecology*, **17**, 5336–5348.

Scoles DR, Collette BB, Graves JE (1998) Global phylogeography of mackerels of the genus *Scomber*. *Fisheries Bulletin*, **96**, 823–842.

Seutin G, White BN, Boag PT (1991) Preservation of avian blood and tissue samples for DNA analyses. *Canadian Journal of Zoology*, **69**, 82–90.

Shackleton N (1987) Oxygen isotopes, ice volume and sea level. *Quaternary Science Reviews*, **6**, 183–190.

Smouse PE, Long JC, Sokal RR (1986) Multiple regression and correlation extensions of the Mantel Test of matrix correspondence. *Systematic Zoology*, **35**, 627–632.

Springer S (1960) Natural history of the sandbar shark, *Eulamia milberti*. *Fishery Bulletin*, **178**, 1–38.

Springer S (1967) Social organization of shark populations. In:*Sharks, skates and ray* (eds Gilbert PW, Mathewson RF, Rall DP), Johns Hopkins Press, Baltimore, MD.

Strasburg JL, Rieseberg LH (2009) How robust are ''Isolation with Migration'' analyses to violations of the IM model? A simulation study. *Molecular Biology and Evolution*, **27**, 297–310.

Thompson JD, Higgins DG, Gibson TJ (1994) CLUSTAL W: improving the sensitivity of progressive multiple sequence alignment through sequence weighting, position-specific gap penalties and weight matrix choice. *Nucleic Acids Research*, **22**, 4673–4680.

Van Oosterhout V, Hutchinson WF, Wills DP, Shipley P (2004) MICRO-CHECKER: software for identifying genotyping errors in microsatellite data. *Molecular Ecology Notes*, **4**, 535–538.

Vermeij GJ, Rosenberg G (1993) Giving and receiving: the tropical Atlantic as donor and recipient region for invading species. *American Malacological Bulletin*, **10**, 181–194.

Verstappen H (1980) Quaternary climactic changes and natural environment in SE Asia. *GeoJournal*, **4**, 45–54.

Wakeley J (2000) The effects of subdivision on the genetic divergence of populations and species. *Evolution*, **54**, 1092–1101.

Waples RS (1998) Separating the wheat from the chaff: patterns of genetic differentiation in high gene flow species. *Journal of Heredity*, **89**, 438–450.

Won Y, Hey J (2005) Divergence population genetics of chimpanzees. *Molecular Biology and Evolution*, **22**, 297–307.

This study was conducted at the Virginia Institute of Marine Science as part of D.S.P.'s dissertation on the population dynamics, reproductive behaviour, and phylogeography of *C. plumbeus*. His research is centred on the conservation genetics of long-lived, exploited marine fishes. J.R.M. is a population geneticist who is interested in the genetic structure, evolution, and conservation of marine populations. E.J.H. is Associate Professor at Southern Illinois University Carbondale and his research interests include a variety of topics involving aspects of the ecology, conservation, systematics, and morphology of marine vertebrates. He serves as Co-chair of the International Union for the Conservation of Nature [IUCN] Shark Specialist group. J.E.G. is head of the fisheries department at VIMS and he studies the processes of molecular evolution in marine organisms, with a focus on the population structure and movements of large pelagic fishes. He is also chair of the U.S. Advisory Committee for the International Commission for the Conservation of Atlantic Tunas.

Supporting information

Additional supporting information may be found in the online version of this article.

Electronic Appendix A Polymorphic nucleotide positions for 67 sandbar shark haplotypes. Only 39 variable sites are displayed, deletions are indicated with (–).

Electronic Appendix B SAMOVA results for groups 2 through 7, MtDNA(1), msat(2). Selected groupings for each run in parenthesis. DF is degrees of freedom, SSD is the sum of squares, VC is the variance component, %V is percent of variance.

Electronic Appendix C Graphical representation of the results from STRUCTURE analyses for number of populations (*k)* = 4. Taiwan is 1, western Australia is 2, Hawaii is 3, eastern Australia is 4, South Africa is 5, Gulf of Mexico is 6, Eastern Shore lagoons of Virginia is 7, Delaware Bay is 8, and Chesapeake Bay is 9. Y axis is proportion of membership. Colors represent each of four clusters to which individual were assigned.

Electronic Appendix D Correspondence analysis of populations using microsatellite data; 1) All regions, 2) Only TW, WAUS and EAUS. Yellow is TW, blue is WAUS, white is EAUS, grey is HI, pink is SAFR, light green is CB, Brown is DEL, Black is ES, and dark green is GOM.

Please note: Wiley-Blackwell are not responsible for the content or functionality of any supporting information supplied by the authors. Any queries (other than missing material) should be directed to the corresponding author for the article.